ELSEVIER

International Journal of Solids and Structures 41 (2004) 2293–2306

INTERNATIONAL JOURNAL OF SOLIDS and STRUCTURES

www.elsevier.com/locate/ijsolstr

On the finite opening of intersonic shear cracks

B. Chen [a], Y. Huang [a,*], H. Gao [b], W. Yang [c]

[a] *Department of Mechanical and Industrial Engineering, University of Illinois at Urbana-Champaign, 1206 West Green Street, Urbana, IL 61801, USA*

[b] *Max Planck Institute for Metals Research, Heisenbergstrasse 3, 70569 Stuttgart, Germany*

[c] *Department of Engineering Mechanics, Tsinghua University, Beijing 100084, China*

Received 3 December 2003; received in revised form 3 December 2003

Abstract

Recent molecular dynamics simulations of dynamic crack propagation have shown that there is a finite crack opening for a shear crack propagating at a sub-Rayleigh speed, but the crack opening becomes significantly smaller once the crack tip velocity exceeds the shear wave speed. To understand this difference between the crack opening for sub-Rayleigh and intersonic shear cracks, we develop in this paper a finite deformation continuum theory incorporating the linear harmonic potential to describe the deformation of a crack in a solid with triangular lattice structure. Using the asymptotic method developed by Knowles [Eng. Fract. Mech. 15 (1981) 469], we show that even after the geometric nonlinearity of finite deformation is accounted for, the intersonic shear cracks have a vanishing crack opening displacement.

© 2003 Elsevier Ltd. All rights reserved.

Keywords: Crack opening; Intersonic crack; Linear harmonic potential

1. Introduction

Rosakis et al. (1999, 2000) conducted the first laboratory experiment of ''intersonic shear cracks'' to show that the velocity of a shear crack propagating along a weak plane in solid could exceed the Rayleigh and shear wave speeds, c_R and c_s, and even approach the dilatational wave speed c_d. The brittle polyester resin was subjected to asymmetric impact in Rosakis et al.'s experiment. The crack rapidly propagated along the weak plane in the polyester resin and shock waves were clearly observed. Rosakis et al.'s experiment (1999, 2000) has motivated the recent atomistic simulations (e.g., Abraham and Gao, 2000) and continuum analyses of intersonic shear crack propagation along weak planes in solids (e.g., Broberg, 1999; Gao et al., 1999; Huang et al., 1999; Needleman, 1999; Needleman and Rosakis, 1999; Yu and Suo, 2000; Gao et al., 2001; Geubelle and Kubair, 2001; Huang and Gao, 2001, 2002; Kubair et al., 2002, 2003; Samudrala et al., 2002a,b). Abraham and Gao (2000) used molecular dynamics (MD) to investigate dynamic crack propagation along a weak interface joining two identical solids subjected to shear-dominated

* Corresponding author. Tel.: +1-217-2655072; fax: +1-217-2446534.
E-mail address: huang9@uiuc.edu (Y. Huang).

0020-7683/$ - see front matter © 2003 Elsevier Ltd. All rights reserved.
doi:10.1016/j.ijsolstr.2003.12.014

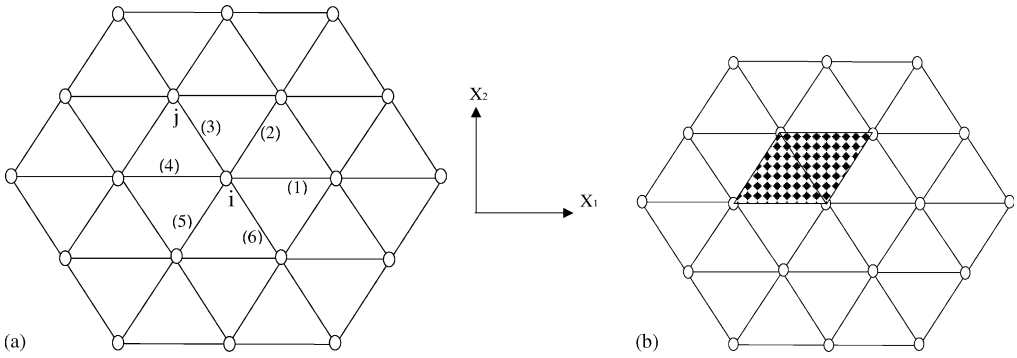

Fig. 1. A schematic diagram of a triangular lattice structure; the lattice direction is X_1; (a) a representative atom and its six nearest-neighbor atoms; (b) the representative volume (shaded area) of each atom.

loading. Their simulations showed a finite crack opening displacement (COD) when the crack propagated at a sub-Rayleigh velocity $v < c_R$. However, once the crack tip velocity exceeded the shear wave speed ($c_s < v < c_d$), the COD became negligible. It is puzzling why the COD for an intersonic crack was negligible while that for a sub-Rayleigh crack was finite under the same loading.

The finite COD for the sub-Rayleigh crack observed in Abraham and Gao's (2000) MD simulations is partially due to the small tensile component they imposed. On the other hand, it is important to note that, even for a pure shear crack, there is finite COD due to the nonlinearity associated with finite deformation (Stephenson, 1982). Knowles (1981) and Geubelle and Knauss (1994) obtained the analytic expression of finite COD for a static shear crack in a nonlinear, generalized Neo-Hookean hyperelastic solid. Recently, Chen et al. (2004) extended Knowles' (1981) analysis to sub-Rayleigh shear crack propagating along weak planes in solids, and also found finite COD, which is consistent with Abraham and Gao's (2000) MD simulations for sub-Rayleigh crack propagation.

In this paper, we investigate the COD of intersonic cracks propagating along weak planes in solids. We focus on intersonic shear cracks since it is well established in continuum dynamic fracture mechanics that tensile (mode-I) cracks cannot propagate at any intersonic speeds (e.g., Freund, 1990; Huang et al., 1999; Rosakis and Huang, 2003), and both Rosakis et al.'s (1999, 2000) experiments and Abraham and Gao's (2000) MD simulations confirm the shear-dominated nature of intersonic cracks. In Section 2, we establish a nonlinear hyperelasticity theory based on the triangular lattice structure (Fig. 1) and the linear harmonic potential used in Abraham and Gao's (2000) MD simulations. We then use the hyperelasticity theory to study the COD of intersonic shear cracks in Section 3, and show that the intersonic shear cracks have vanishing COD, which is consistent with the negligible COD in Abraham and Gao's MD simulations.

2. A nonlinear hyperelasticity theory incorporating the linear harmonic potential

Fig. 1a shows the triangular lattice structure in Abraham and Gao's MD simulations. The interaction between atoms was characterized by a linear harmonic potential. A plane-stress constitutive relation is established in this section from the same triangular lattice structure and linear harmonic potential. The plane-stress condition is consistent with Abraham and Gao's (2000) two-dimensional MD simulations of a single layer of atoms, though the present approach can be straightforwardly extended to plane-strain or three-dimensional deformation.

2.1. The linear harmonic potential

The interaction between atoms is characterized by a linear harmonic potential φ, which gives the energy stored in an atomic bond (pair of atoms)

$$\varphi(l_{ij}) = \frac{1}{2}k(l_{ij} - l_0)^2, \tag{1}$$

where k is the linear spring constant, l_{ij} is the distance between atoms i and j, and l_0 is the equilibrium bond length. Its derivative $\frac{\partial\varphi}{\partial l_{ij}} = k(l_{ij} - l_0)$ gives the force between atoms i and j, which is linearly proportional to the stretched bond length $l_{ij} - l_0$.

2.2. Deformation of an atomic bond

Let $\mathbf{X}$ and $\mathbf{x} = \mathbf{X} + \mathbf{U}$ denote the positions of a material point in the reference (undeformed) and current (deformed) configurations, respectively, where $\mathbf{U}$ is the displacement. The deformation gradient $\mathbf{F}$ is given by

$$\mathbf{F} = \mathbf{I} + \frac{\partial \mathbf{U}}{\partial \mathbf{X}}, \tag{2}$$

where $\mathbf{I}$ is the second-order identity tensor. The Green–Lagrange strain $\mathbf{E}$ at $\mathbf{X}$ is related to the deformation gradient $\mathbf{F} = \frac{\partial \mathbf{x}}{\partial \mathbf{X}}$ by

$$\mathbf{E} = \tfrac{1}{2}(\mathbf{F}^{\mathbf{T}} \cdot \mathbf{F} - \mathbf{I}), \tag{3}$$

where $\mathbf{F}^{\mathbf{T}}$ is the transpose of $\mathbf{F}$.

Let $\xi^{(\mathbf{n})}$ denote the unit vector of the nth bond ($n = 1, 2, \ldots$) at $\mathbf{X}$, and l_0 the corresponding equilibrium bond length in the reference (undeformed) configuration. For the triangular lattice structure in Fig. 1a, each atom interacts with six nearest-neighbor atoms and the bond directions in the reference (undeformed) configuration are $\xi^{(\mathbf{1})} = -\xi^{(\mathbf{4})} = (1, 0)$, $\xi^{(\mathbf{2})} = -\xi^{(\mathbf{5})} = (\frac{1}{2}, \frac{\sqrt{3}}{2})$, and $\xi^{(\mathbf{3})} = -\xi^{(\mathbf{6})} = (-\frac{1}{2}, \frac{\sqrt{3}}{2})$, where X_1 is parallel to a bond (Fig. 1). The length of the stretched bond is related to the strain $\mathbf{E}$ by

$$l^{(n)} = l_0\sqrt{1 + 2\xi_I^{(n)}E_{IJ}\xi_J^{(n)}}, \tag{4}$$

or

$$\begin{aligned} l^{(1)} &= l^{(4)} = l_0\sqrt{1 + 2E_{11}}, \\ l^{(2)} &= l^{(5)} = l_0\sqrt{1 + \frac{E_{11}}{2} + \frac{3}{2}E_{22} + \frac{\sqrt{3}}{2}(E_{12} + E_{21})}, \\ l^{(3)} &= l^{(6)} = l_0\sqrt{1 + \frac{E_{11}}{2} + \frac{3}{2}E_{22} - \frac{\sqrt{3}}{2}(E_{12} + E_{21})}. \end{aligned} \tag{5}$$

2.3. Continuum strain energy density

For the linear harmonic potential (1), the energy stored in the nth bond is $\varphi^{(n)} = \frac{1}{2}k[l^{(n)} - l_0]^2$. Based on the Cauchy–Born rule (e.g., Milstein, 1980; Gao, 1996; Tadmor et al., 1996; Gao and Klein, 1998; Zhang et al., 2002a,b,c; Huang and Wang, 2003), the continuum strain energy density Φ can be obtained from the energy stored in all six atomic bonds at $\mathbf{X}$ as

$$\Phi = \frac{1}{2}\frac{\sum_{n=1}^{6}\varphi^{(n)}}{V}, \tag{6}$$

where the factor 1/2 results from the equal split of energy between two atoms in each bond, $V = \frac{\sqrt{3}}{2} l_0^2 t_0$ is the representative volume for each atom, as illustrated by the shaded area in Fig. 1b, l_0 is the equilibrium bond length prior to deformation, and t_0 is the thickness in the out-of-plane direction which does not enter the continuum theory once the shear modulus is known, as shown in the following.

2.4. The constitutive model based on the linear harmonic potential

The second Piola–Kirchhoff stress **S** is the work conjugate of the Green–Lagrange strain and it can be obtained from the strain energy density Φ by

$$S_{IJ} = \frac{\partial \Phi}{\partial E_{IJ}} = \frac{1}{\sqrt{3}t_0}\sum_{n=1}^{6}\frac{\varphi'[l^{(n)}]}{l^{(n)}}\xi_I^{(n)}\xi_J^{(n)} = \frac{k}{\sqrt{3}t_0}\sum_{n=1}^{6}\frac{l^{(n)}-l_0}{l^{(n)}}\xi_I^{(n)}\xi_J^{(n)}.$$

Its components are

$$\begin{aligned}
S_{11} &= \frac{2k}{\sqrt{3}t_0}\left[\frac{3}{2} - \frac{l_0}{l^{(1)}} - \frac{l_0}{4l^{(2)}} - \frac{l_0}{4l^{(3)}}\right],\\
S_{22} &= \frac{2k}{\sqrt{3}t_0}\left[\frac{3}{2} - \frac{3}{4}\frac{l_0}{l^{(2)}} - \frac{3}{4}\frac{l_0}{l^{(3)}}\right],\\
S_{12} &= \frac{2k}{\sqrt{3}t_0}\left[-\frac{\sqrt{3}}{4}\frac{l_0}{l^{(2)}} + \frac{\sqrt{3}}{4}\frac{l_0}{l^{(3)}}\right],
\end{aligned} \tag{7}$$

where $l^{(1)}$, $l^{(2)}$, and $l^{(3)}$ depend on the strain E_{IJ} via (5). Eq. (7) gives a *nonlinear*, *anisotropic* stress–strain relation, even though it is based on the *linear* harmonic potential. The nonlinearity and anisotropy come merely from the finite deformation.

For an infinitesimal deformation, $|E_{IJ}| << 1$, (7) degenerates to the following linear elastic and isotropic relation,

$$\begin{aligned}
S_{11} &= \frac{3\sqrt{3}k}{4t_0}\left(E_{11} + \frac{1}{3}E_{22}\right),\\
S_{22} &= \frac{3\sqrt{3}k}{4t_0}\left(E_{22} + \frac{1}{3}E_{11}\right),\\
S_{12} &= \frac{\sqrt{3}k}{2t_0}E_{12},
\end{aligned}$$

which gives the shear modulus $\mu = \frac{\sqrt{3}k}{4t_0}$, and Poisson's ratio $v = \frac{1}{3}$. Once the shear modulus μ is specified, the linear spring constant k and thickness t_0 do not enter the constitutive relation (7) anymore since the coefficient $\frac{2k}{\sqrt{3}t_0}$ in (7) equals $\frac{8}{3}\mu$. The constitutive relation (7) is also independent of the equilibrium bond length l_0 after proper normalization.

2.5. Equation of motion and boundary conditions

The equation of motion is

$$(\mathbf{F}\cdot\mathbf{S})\cdot\nabla = \rho_0\frac{\partial^2\mathbf{U}}{\partial t^2}, \tag{8}$$

where t is the time, $\rho_0 = \frac{m}{V}$ is the mass density in the reference (undeformed) configuration given in terms of the atomic mass m and representative volume V for each atom, and ∇ is the gradient operator in the reference configuration. For a steady-state crack propagation along the X_1 direction, the acceleration $\frac{\partial^2 \mathbf{U}}{\partial t^2} = v^2 \frac{\partial^2 \mathbf{U}}{\partial \mathbf{X}_1^2}$, where v is the crack tip velocity. Eq. (8) becomes

$$(\mathbf{F} \cdot \mathbf{S}) \cdot \nabla = \rho_0 v^2 \frac{\partial^2 \mathbf{U}}{\partial \mathbf{X}_1^2}. \tag{9}$$

The traction-free boundary condition on the crack faces is

$$(\mathbf{F} \cdot \mathbf{S}) \cdot \mathbf{N} = \mathbf{0}, \tag{10}$$

where $\mathbf{N}$ is the unit normal of the crack faces in the reference (undeformed) configuration.

3. Crack opening displacement of an intersonic shear crack

Knowles (1981) and Geubelle and Knauss (1994) studied the finite COD of a static shear crack in a nonlinear, generalized Neo-Hookean hyperelastic solid. A semi-infinite crack in an infinite solid was subject to a remote classical linear elastic K_{II} field. The material surrounding the crack tip was divided into three regions, as illustrated in Fig. 2. There was an *inner region* in the immediate vicinity of the crack tip within which the nonlinear effect dominated and the field was completely different from the classical linear elastic

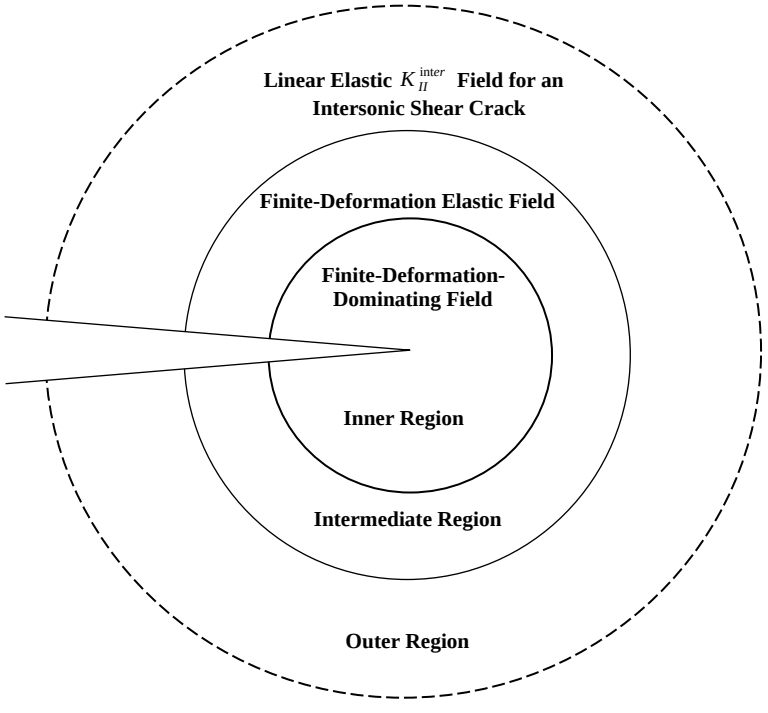

Fig. 2. A schematic diagram of different zones surrounding the crack tip, including the inner region in which the effect of finite deformation dominates; the intermediate region in which the finite deformation effect is significant and comparable to the classical linear elastic asymptotic $K_{\mathrm{II}}^{\mathrm{inter}}$ field for an intersonic shear crack; and the outer region where the effect of finite deformation vanishes and the field degenerates to the classical $K_{\mathrm{II}}^{\mathrm{inter}}$ field.

K_{II} field. The inner region was surrounded by an *intermediate region* within which the nonlinear effect was significant but not dominant, and the field in the intermediate region was a perturbation to the linear elastic K_{II} field. The intermediate region was in turn surrounded by an *outer region* within which the nonlinear effect was negligible and the field degenerated to the remote classical linear elastic K_{II} field. Knowles (1981) obtained the analytic solution in the intermediate region, while Geubelle and Knauss (1994) obtained the solution in the inner region. Both showed finite COD for static shear cracks. Chen et al. (2004) investigated sub-Rayleigh propagation of a shear crack along a weak plane in a solid characterized by the constitutive law (7), and they also found finite COD in the intermediate region.

We investigate the possibility of finite COD of an intersonic shear crack propagating with velocity $v(> c_s)$ along a weak plane in an infinite solid. The solid is characterized by the nonlinear, anisotropic constitutive relation (7). We follow the same approach as Knowles (1981) and Chen et al. (2004) to divide the material surrounding the (moving) crack tip into the inner, intermediate, and outer regions (Fig. 2), and focus on the solution in the intermediate region. The classical linear elastic asymptotic field for an intersonic shear crack (e.g., Freund, 1990) is imposed as the remote boundary condition.

3.1. Displacement in the outer region: the classical linear elastic asymptotic field for an intersonic shear crack

The solution in the outer region is the classical linear elastic asymptotic field for an intersonic shear crack. The stress has the singularity $1/r^q$ (e.g., Freund, 1990; Samudrala et al., 2002a,b), where

$$q = \frac{1}{\pi}\tan^{-1}\frac{4\hat{\alpha}_s\alpha_d}{(1-\hat{\alpha}_s^2)^2} \tag{11}$$

is the power of stress singularity, r is the distance to the moving crack tip, $\hat{\alpha}_s = \left(\frac{v^2}{c_s^2}-1\right)^{1/2}$ and $\alpha_d = \left(1-\frac{v^2}{c_d^2}\right)^{1/2}$ are functions of the crack tip velocity v, and c_s and $c_d = \sqrt{3}c_s$ are the shear and dilatational wave speeds, respectively. The power of stress singularity q is always less than 1/2 for intersonic crack propagation except $v = \sqrt{2}c_s$ at which $q = 1/2$ such that the intersonic crack tip resumes the conventional square-root singularity. The classical linear elastic asymptotic field is characterized by an intersonic (shear) stress intensity factor $K_{II}^{inter} = \sqrt{2\pi}r^q\sigma_{12}|_{\theta=0}$ (Samudrala et al., 2002a,b), where σ_{12} is the shear stress, θ is the polar angle measured from the moving crack with $\theta = \pm\pi$ being the crack faces.

The displacements in the asymptotic field have anti-symmetry $U_r(r,\theta) = -U_r(r,-\theta)$ and $U_\theta(r,\theta) = U_\theta(r,-\theta)$ in polar coordinates (r,θ). The displacements in the upper half plane $(0 \leqslant \theta \leqslant \pi)$ are given by

$$U_\alpha = \frac{K_{II}^{inter}}{\mu}r^{1-q}\overline{U}_\alpha(\theta) \quad (\alpha = r,\theta), \tag{12}$$

where $\theta = \pi$ corresponds to upper crack face, $\overline{U}_r$ and $\overline{U}_\theta$ are angular functions given in the following

$$\begin{Bmatrix}\overline{U}_r\\ \overline{U}_\theta\end{Bmatrix} = \begin{Bmatrix}\cos\theta & \sin\theta\\ -\sin\theta & \cos\theta\end{Bmatrix}\begin{Bmatrix}\overline{U}_1\\ \overline{U}_2\end{Bmatrix}, \tag{13}$$

$$\begin{Bmatrix}\overline{U}_1\\ \overline{U}_2\end{Bmatrix} = \frac{1}{4\sqrt{2\pi}(1-q)\alpha_d}\begin{Bmatrix}2k_d^{1-q}\sin(1-q)\theta_d - (1-\hat{\alpha}_s^2)\sin q\pi|\cos\theta + \hat{\alpha}_s\sin\theta|^{1-q}H(\theta-\theta_q)\\ 2\alpha_d k_d^{1-q}\cos(1-q)\theta_d + \frac{1-\hat{\alpha}_s^2}{\hat{\alpha}_s}\sin q\pi|\cos\theta + \hat{\alpha}_s\sin\theta|^{1-q}H(\theta-\theta_q)\end{Bmatrix} \tag{14}$$

are angular functions of Cartesian components U_1 and U_2 of the displacements (Freund, 1990; Samudrala et al., 2002a,b); θ_d and k_d are functions of polar angle θ and crack tip velocity v given by

$$\theta_{\mathrm{d}} = \tan^{-1}(\alpha_{\mathrm{d}} \tan\theta), \quad k_{\mathrm{d}} = \left(1 - \frac{v^2}{c_{\mathrm{d}}^2} \sin^2\theta\right)^{1/2} \tag{15}$$

and θ_{d} ranges from 0 to π. The function H in (14) is the unit step function, which equals unity for $\theta \geqslant \theta_q$ and 0 for $\theta < \theta_q$. It is discontinuous across the shock wave angle $\theta_q = \pi - \tan^{-1}\frac{1}{\hat{\alpha}_{\mathrm{s}}}$, where θ_q ranges from $\pi/2$ (90°, for $v = c_{\mathrm{s}}$) to $\pi - \tan^{-1}\frac{1}{\sqrt{2}}$ (144.7°, for $v = c_{\mathrm{d}} = \sqrt{3}c_{\mathrm{s}}$). It is observed that, at the special crack tip velocity $v = \sqrt{2}c_{\mathrm{s}}$ which gives the conventional square-root singularity $q = 1/2$ in (11), the shock waves disappear since the coefficient $1 - \hat{\alpha}_{\mathrm{s}}^2$ of the unit step function H in (14) vanishes.

3.2. Jump condition across the shock wave

It can be verified that the displacements in (12) are continuous across the shock wave at $\theta = \theta_q$, but the velocity and stress suffer strong discontinuity for $v \neq \sqrt{2}c_{\mathrm{s}}$.

For a shock wave travelling with velocity $v(> c_{\mathrm{s}})$ and shock wave angle θ_q, the jump condition across the discontinuity (shock wave) is (e.g., Abeyaratne and Knowles, 1990)

$$\rho_0 v \sin\theta_q [\![\dot{\mathbf{U}}]\!] - [\![\mathbf{F}\cdot\mathbf{S}]\!]\cdot\mathbf{e}_\theta = \mathbf{0}, \tag{16}$$

where ρ_0 is the mass density in the reference (undeformed) configuration, $\dot{\mathbf{U}} = \frac{\partial \mathbf{U}}{\partial t}$ is the material velocity, $\mathbf{F}$ and $\mathbf{S}$ are the deformation gradient and second Piola–Kirchhoff stress, respectively, and $\mathbf{e}_\theta$ is the base vector in the circumferential direction on the shock wave ($\theta = \theta_q$). It can be verified that the velocity, deformation gradient, and stress fields obtained from the displacement in (12) for the classical linear elastic asymptotic field of an intersonic shear crack satisfy the above jump condition.

3.3. Displacement in the intermediate region

Following Knowles (1981) and Chen et al. (2004), we seek the solution in the intermediate region that represents a perturbation to the outer-region field in (12), i.e.,

$$\begin{Bmatrix} U_r \\ U_\theta \end{Bmatrix} = \frac{K_{\mathrm{II}}^{\mathrm{inter}}}{\mu} r^{1-q} \begin{Bmatrix} \overline{U}_r(\theta) \\ \overline{U}_\theta(\theta) \end{Bmatrix} + r^{1-p} \begin{Bmatrix} \overline{V}_r(\theta) \\ \overline{V}_\theta(\theta) \end{Bmatrix} + \mathrm{o}(r^{1-p}) \tag{17}$$

for large r, where the perturbed terms, on the order of r^{1-p}, result from nonlinearity associated with finite deformation; the exponent p and angular functions $\overline{V}_r$ and $\overline{V}_\theta$ are to be determined, and

$$p > q \tag{18}$$

in order to ensure that (17) degenerates to (12) as the outer region is approached ($r \to \infty$); $\mathrm{o}(r^{1-p})$ in (17) represents terms that are negligible as compared to r^{1-p} for large r.

The deformation gradient $\mathbf{F}$ is obtained straightforwardly by substituting the displacement in (17) into (2),

$$\begin{Bmatrix} F_{rr} \\ F_{r\theta} \\ F_{\theta r} \\ F_{\theta\theta} \end{Bmatrix} = \begin{Bmatrix} 1 \\ 0 \\ 0 \\ 1 \end{Bmatrix} + \frac{K_{\mathrm{II}}^{\mathrm{inter}}}{\mu r^q} \begin{Bmatrix} \overline{F}_{rr}(\theta) \\ \overline{F}_{r\theta}(\theta) \\ \overline{F}_{\theta r}(\theta) \\ \overline{F}_{\theta\theta}(\theta) \end{Bmatrix} + r^{-p} \begin{Bmatrix} 1 - p\overline{V}_r \\ \overline{V}_r' - \overline{V}_\theta \\ 1 - p\overline{V}_\theta \\ \overline{V}_\theta' + \overline{V}_r \end{Bmatrix} + \mathrm{o}(r^{-p}), \tag{19}$$

where $\overline{F}_{rr} = (1-q)\overline{U}_r$, $\overline{F}_{r\theta} = \overline{U}_r' - \overline{U}_\theta$, $\overline{F}_{\theta r} = (1-q)\overline{U}_\theta$, and $\overline{F}_{\theta\theta} = \overline{U}_\theta' + \overline{U}_r$ are angular functions of the deformation gradient $\mathbf{F}$ in the classical linear elastic asymptotic field for an intersonic shear crack, $\overline{U}_r' = \frac{\mathrm{d}\overline{U}_r}{\mathrm{d}\theta}$ and $\overline{U}_\theta' = \frac{\mathrm{d}\overline{U}_\theta}{\mathrm{d}\theta}$ are obtained from (13); and $\overline{V}_r' = \frac{\mathrm{d}\overline{V}_r}{\mathrm{d}\theta}$ and $\overline{V}_\theta' = \frac{\mathrm{d}\overline{V}_\theta}{\mathrm{d}\theta}$. The Green–Lagrange strain $\mathbf{E}$ in (3) and stretched bond lengths $l^{(1)}$, $l^{(2)}$, and $l^{(3)}$ in (5) can be similarly expanded in terms of r. In addition to r^{-q} and

r^{-p}, they involve r^{-2q} terms resulting from $\mathbf{F}^{\mathbf{T}} \cdot \mathbf{F}$ in (3). The second Piola–Kirchhoff stress $\mathbf{S}$ is then obtained from (7) as

$$\begin{aligned}
S_{rr} &= \frac{K_{\mathrm{II}}^{\mathrm{inter}}}{r^q}\overline{S}_{rr}(\theta) + \mu r^{-p}\left[\overline{V}'_\theta + (4-3p)\overline{V}_r\right] + \frac{(K_{\mathrm{II}}^{\mathrm{inter}})^2}{\mu r^{2q}}\overline{S}_{rr}^{\mathrm{FD}}(\theta) + \mathrm{o}(r^{-2q}, r^{-p}),\\
S_{r\theta} = S_{\theta r} &= \frac{K_{\mathrm{II}}^{\mathrm{inter}}}{r^q}\overline{S}_{r\theta}(\theta) + \mu r^{-p}\left[\overline{V}'_r - p\overline{V}_\theta\right] + \frac{(K_{\mathrm{II}}^{\mathrm{inter}})^2}{\mu r^{2q}}\overline{S}_{r\theta}^{\mathrm{FD}}(\theta) + \mathrm{o}(r^{-2q}, r^{-p}),\\
S_{\theta\theta} &= \frac{K_{\mathrm{II}}^{\mathrm{inter}}}{r^q}\overline{S}_{\theta\theta}(\theta) + \mu r^{-p}\left[3\overline{V}'_\theta + (4-p)\overline{V}_r\right] + \frac{(K_{\mathrm{II}}^{\mathrm{inter}})^2}{\mu r^{2q}}\overline{S}_{\theta\theta}^{\mathrm{FD}}(\theta) + \mathrm{o}(r^{-2q}, r^{-p}),
\end{aligned} \tag{20}$$

where the leading, $\frac{1}{r^q}$ terms correspond to the classical linear elastic asymptotic field for an intersonic shear crack (Freund, 1990), $\overline{S}_{rr} = 3\overline{F}_{rr} + \overline{F}_{\theta\theta}$, $\overline{S}_{r\theta} = \overline{F}_{r\theta} + \overline{F}_{\theta r}$, and $\overline{S}_{\theta\theta} = \overline{F}_{rr} + 3\overline{F}_{\theta\theta}$ are the corresponding angular functions; the $\frac{1}{r^{2q}}$ terms result from finite deformation [i.e., $\mathbf{F}^{\mathbf{T}} \cdot \mathbf{F}$ in (3)], and $\overline{S}_{IJ}^{\mathrm{FD}}(\theta)$ are the corresponding angular functions that are known in terms of $\overline{U}_r$ and $\overline{U}_\theta$; and $\mathrm{o}(r^{-2q}, r^{-p})$ represents terms that are negligible as compared to either r^{-2q} or r^{-p} for large r.

For a steady-state intersonic shear crack propagating with velocity $v(> c_{\mathrm{s}})$, the acceleration in (9) can be written in terms of the displacement in (17) as

$$\begin{aligned}
\frac{\partial^2 \mathbf{U}}{\partial t^2} = v^2\frac{\partial^2 \mathbf{U}}{\partial X_{\mathrm{I}}^2} = v^2\frac{K_{\mathrm{II}}^{\mathrm{inter}}}{r^{1+q}}\mathbf{a}(\theta) &+ \mathbf{e}_{\mathbf{r}}v^2 r^{-p-1}\Big\{-\cos^2\theta p(1-p)\overline{V}_r + \sin^2\theta\left[\overline{V}''_r - p\overline{V}_r - 2\overline{V}'_\theta\right]\\
&+ p\sin 2\theta\left(\overline{V}'_r - \overline{V}_\theta\right)\Big\} + \mathbf{e}_\theta v^2 r^{-p-1}\Big\{-\cos^2\theta p(1-p)\overline{V}_\theta\\
&+ \sin^2\theta\left[\overline{V}''_\theta - p\overline{V}_\theta + 2\overline{V}'_r\right] + p\sin 2\theta\left(\overline{V}'_\theta + \overline{V}_r\right)\Big\} + \mathrm{o}(r^{-p-1}),
\end{aligned} \tag{21}$$

where the leading, $\frac{1}{r^{1+q}}$ term corresponds to the linear elastic asymptotic field for an intersonic shear crack, $\mathbf{a}(\theta)$ is the corresponding angular function that is known in terms of $\overline{U}_r$ and $\overline{U}_\theta$; and $\mathbf{e}_{\mathbf{r}}$ and $\mathbf{e}_\theta$ are the base vectors in the moving coordinates. The substitution of deformation gradient (19), second Piola–Kirchhoff stress (20), and acceleration (21) into the equation of motion (9) yields the following equations for $\overline{V}_r$ and $\overline{V}_\theta$,

$$\begin{aligned}
&\left[\left(1-\frac{v^2}{c_{\mathrm{s}}^2}\sin^2\theta\right)\frac{\mathrm{d}}{\mathrm{d}\theta} - p\frac{v^2}{c_{\mathrm{s}}^2}\sin 2\theta\right]\left(\overline{V}'_r - \overline{V}_\theta\right) - \left(1+2p-\frac{v^2}{c_{\mathrm{s}}^2}\sin^2\theta\right)\left(\overline{V}'_\theta + \overline{V}_r\right)\\
&\quad + (1-p)\left[1-3p+\frac{v^2}{c_{\mathrm{s}}^2}(\cos 2\theta - (1-p)\cos^2\theta)\right]\overline{V}_r = r^{p-2q}\frac{(K_{\mathrm{II}}^{\mathrm{inter}})^2}{\mu^2}\bar{f}_r(\theta) + \mathrm{o}(1, r^{p-2q}),\\
&\left[\left(3-\frac{v^2}{c_{\mathrm{s}}^2}\sin^2\theta\right)\frac{\mathrm{d}}{\mathrm{d}\theta} - p\frac{v^2}{c_{\mathrm{s}}^2}\sin 2\theta\right]\left(\overline{V}'_\theta + \overline{V}_r\right) + \left(3-2p-\frac{v^2}{c_{\mathrm{s}}^2}\sin^2\theta\right)\left(\overline{V}'_r - \overline{V}_\theta\right)\\
&\quad + (1-p)\left[3-p+\frac{v^2}{c_{\mathrm{s}}^2}(\cos 2\theta - (1-p)\cos^2\theta)\right]\overline{V}_\theta = r^{p-2q}\frac{(K_{\mathrm{II}}^{\mathrm{inter}})^2}{\mu^2}\bar{f}_\theta(\theta) + \mathrm{o}(1, r^{p-2q}),
\end{aligned} \tag{22}$$

where $\bar{f}_r$ and $\bar{f}_\theta$ are the angular functions scaling with $\frac{(K_{\mathrm{II}}^{\mathrm{inter}})^2}{\mu^2}$ in the equation of motion due to finite deformation, and they are known in terms of $\overline{U}_r$ and $\overline{U}_\theta$; $\bar{f}_r$ and $\bar{f}_\theta$ are even and odd functions of θ, respectively; $\mathrm{o}(1, r^{p-2q})$ in (22) represent terms that are negligible as compared to unity or r^{p-2q} for large r. It is observed that the left hand sides of the above equations depend on θ while the right hand sides may depend on r. Its implication will be discussed in the next Section 3.4.

The crack-face traction-free boundary conditions (10) become

$$\begin{aligned} &3\overline{V}_\theta' + (4-p)\overline{V}_r = r^{p-2q}\frac{(K_{\mathrm{II}}^{\mathrm{inter}})^2}{\mu^2}(\cdots) + o(1, r^{p-2q}) \quad \text{at } \theta = \pm\pi, \\ &\overline{V}_r' - p\overline{V}_\theta = r^{p-2q}\frac{(K_{\mathrm{II}}^{\mathrm{inter}})^2}{\mu^2}(\cdots) + o(1, r^{p-2q}) \quad \text{at } \theta = \pm\pi, \end{aligned} \tag{23}$$

where $(\cdots)$ represent the coefficients that scale with $\frac{(K_{\mathrm{II}}^{\mathrm{inter}})^2}{\mu^2}$, which are known in terms of $\overline{U}_r(\pi)$, $\overline{U}_\theta(\pi)$, $\overline{U}_r'(\pi)$ and $\overline{U}_\theta'(\pi)$ but are not presented here because of their rather long and tedious expressions.

3.4. Vanishing crack opening displacement in the intermediate region

We show in this section that an intersonic shear crack must have a vanishing COD in the intermediate region. For the exponent $p > q$ as required in (17) for large r, there are four possible combinations of q and p, as discussed separately in the following.

(i) $p > 2q$

The terms $r^{p-2q}\frac{(K_{\mathrm{II}}^{\mathrm{inter}})^2}{\mu^2}\bar{f}_r$ and $r^{p-2q}\frac{(K_{\mathrm{II}}^{\mathrm{inter}})^2}{\mu^2}\bar{f}_\theta$ on the right hand sides become the dominant terms in (22) for large r such that $\overline{V}_r$ and $\overline{V}_\theta$ on the left hand sides of (22) are negligible. Eq. (22) then gives $\bar{f}_r = \bar{f}_\theta = 0$, which do not involve the unknown functions $\overline{V}_r$ and $\overline{V}_\theta$ anymore. Since $\bar{f}_r$ and $\bar{f}_\theta$ are known in terms of $\overline{U}_r$ and $\overline{U}_\theta$, $\bar{f}_r = \bar{f}_\theta = 0$ impose additional constraints on the angular functions $\overline{U}_r$ and $\overline{U}_\theta$ for all θ between 0 and π. It can be verified that such constraints cannot be met. Therefore, $p > 2q$ is not possible.

(ii) $p < 2q$

The range of p is $q < p < 2q$. The terms $r^{p-2q}\frac{(K_{\mathrm{II}}^{\mathrm{inter}})^2}{\mu^2}\bar{f}_r$ and $r^{p-2q}\frac{(K_{\mathrm{II}}^{\mathrm{inter}})^2}{\mu^2}\bar{f}_\theta$ on the right hand sides of (22) become negligible for large r, and (22) gives the following linear, homogeneous ordinary differential equations for $\overline{V}_r$ and $\overline{V}_\theta$,

$$\begin{aligned} &\left[\left(1-\frac{v^2}{c_s^2}\sin^2\theta\right)\frac{\mathrm{d}}{\mathrm{d}\theta} - p\frac{v^2}{c_s^2}\sin 2\theta\right]\left(\overline{V}_r' - \overline{V}_\theta\right) - \left(1+2p-\frac{v^2}{c_s^2}\sin^2\theta\right)\left(\overline{V}_\theta' + \overline{V}_r\right) \\ &\quad + (1-p)\left[1-3p+\frac{v^2}{c_s^2}(\cos 2\theta - (1-p)\cos^2\theta)\right]\overline{V}_r = 0, \\ &\left[\left(3-\frac{v^2}{c_s^2}\sin^2\theta\right)\frac{\mathrm{d}}{\mathrm{d}\theta} - p\frac{v^2}{c_s^2}\sin 2\theta\right]\left(\overline{V}_\theta' + \overline{V}_r\right) + \left(3-2p-\frac{v^2}{c_s^2}\sin^2\theta\right)\left(\overline{V}_r' - \overline{V}_\theta\right) \\ &\quad + (1-p)\left[3-p+\frac{v^2}{c_s^2}(\cos 2\theta - (1-p)\cos^2\theta)\right]\overline{V}_\theta = 0. \end{aligned} \tag{24}$$

Similarly, the crack-face traction-free boundary conditions (23) become

$$\begin{aligned} &3\overline{V}_\theta' + (4-p)\overline{V}_r = 0 \quad \text{at } \theta = \pm\pi, \\ &\overline{V}_r' - p\overline{V}_\theta = 0 \quad \text{at } \theta = \pm\pi, \end{aligned} \tag{25}$$

which are also linear and homogeneous. Eqs. (24) and (25) have the trivial solution $\overline{V}_r = \overline{V}_\theta = 0$, which gives vanishing COD. The non-trivial solutions of (24) and (25) can be obtained analytically following the same approach as that for the classical linear elastic asymptotic field of an intersonic shear crack (e.g., Freund, 1990). The exponent p serves as the eigenvalue of the homogeneous ordinary differential equations (24) with homogeneous boundary conditions (25), and its solution is

$$p = \frac{n}{2} + q, \quad n = 0, \pm 1, \pm 2, \pm 3, \ldots, \tag{26}$$

where $n = 0$ (i.e., $p = q$) corresponds to the classical linear elastic asymptotic field for an intersonic shear crack (Freund, 1990). It is straightforward to verify that none of the exponents p above satisfy $q < p < 2q$. Therefore, $p < 2q$ does not give a finite, non-vanishing COD in the intermediate region.

(iii) $p = 2q$ and $q < 1/2$

For $q < 1/2$ (i.e., crack tip velocity $v \neq \sqrt{2}c_s$), there exist shock waves emanating from the intersonic crack tip. We show in the following that, for $p = 2q$, the jump condition (16) across the shock wave cannot be satisfied. The radial component (i.e., along r direction) of the jump condition (16) gives

$$\rho_0 v \sin\theta_q [\![\dot{U}_r]\!] = [\![F_{rr}S_{r\theta} + F_{r\theta}S_{\theta\theta}]\!]. \tag{27}$$

The jump $[\![\dot{U}_r]\!]$ can be obtained from (17) and the steady-state condition $\frac{\partial}{\partial t} = -v\frac{\partial}{\partial X_1}$ as

$$[\![\dot{U}_r]\!] = \frac{vK_{\mathrm{II}}^{\mathrm{inter}}}{\mu r^q}\sin\theta_q [\![\overline{U}'_r]\!] + \frac{v}{r^{2q}}\sin\theta_q [\![\overline{V}'_r]\!], \tag{28}$$

where we have used $[\![\overline{U}_r]\!] = [\![\overline{U}_\theta]\!] = [\![\overline{V}_r]\!] = [\![\overline{V}_\theta]\!] = 0$ across the shock wave angle $\theta = \theta_q$, and $p = 2q$. The right hand side of (27) is obtained from (19) and (20) as

$$[\![F_{rr}S_{r\theta} + F_{r\theta}S_{\theta\theta}]\!] = \frac{K_{\mathrm{II}}^{\mathrm{inter}}}{r^q}[\![\overline{S}_{r\theta}]\!] + \frac{\mu}{r^{2q}}[\![\overline{V}'_r]\!] + \frac{(K_{\mathrm{II}}^{\mathrm{inter}})^2}{\mu r^{2q}}[\![\overline{S}_{r\theta}^{\mathrm{FD}}]\!] + \frac{(K_{\mathrm{II}}^{\mathrm{inter}})^2}{\mu r^{2q}}[\![\overline{F}_{rr}\overline{S}_{r\theta} + \overline{F}_{r\theta}\overline{S}_{\theta\theta}]\!], \tag{29}$$

where $\overline{F}_{rr}$, $\overline{F}_{r\theta}$, $\overline{S}_{r\theta}$, $\overline{S}_{\theta\theta}$, and $\overline{S}_{r\theta}^{\mathrm{FD}}$ are angular functions in (19) and (20). The substitution of (28) and (29) into the jump condition (27) yields the following relation that does not involve $\overline{V}_r$ and $\overline{V}_\theta$,

$$[\![\overline{S}_{r\theta}^{\mathrm{FD}} + \overline{F}_{rr}\overline{S}_{r\theta} + \overline{F}_{r\theta}\overline{S}_{\theta\theta}]\!] = 0. \tag{30}$$

Since the functions in (30) are known in terms of $\overline{U}_r$ and $\overline{U}_\theta$, the above equation imposes an additional constraint on $\overline{U}_r$ and $\overline{U}_\theta$, which cannot be satisfied. In fact, using Mathematica, we have expressed (30) as

$$-\frac{1}{2}\sin 6\theta_q [\![\overline{U}'_r 2]\!] + g(\theta_q)[\![\overline{U}'_r]\!] = 0, \tag{31}$$

where

$$g(\theta_q) = q\sin 6\theta_q \overline{U}_\theta(\theta_q) + (2 - \cos 6\theta_q)\overline{U}'_\theta(\theta_q) + (4 - 2q - q\cos 6\theta_q)\overline{U}_r(\theta_q) \tag{32}$$

is a continuous function of θ_q because $\overline{U}_r$, $\overline{U}_\theta$ and $\overline{U}'_\theta$ are continuous at $\theta = \theta_q$. It can be verified from (13) and (14) that $[\![\overline{U}'_\theta]\!] = 0$ at $\theta = \theta_q$, and $[\![\overline{U}'_r]\!]$ and $[\![\overline{U}'_r 2]\!]$ have singular jumps on the order of $|\theta - \theta_q|^{-q}$ and $|\theta - \theta_q|^{-2q}$, respectively. For the jump condition (31) to hold, both coefficients $\sin 6\theta_q$ and $g(\theta_q)$ must vanish simultaneously. We have verified that there is no θ_q between $\pi/2$ and π that satisfies $\sin 6\theta_q = g(\theta_q) = 0$. Therefore, $p = v$ and $q < 1/2$ is not possible.

(iv) $p = 2q$ and $q = 1/2$ (therefore $p = 1$)

As discussed in Section 3.1, there exists only one crack tip velocity that gives $q = 1/2$, i.e., $v = \sqrt{2}c_s$, at which the shock waves disappear and jump condition (16) is satisfied automatically. At this special crack tip velocity, $\widehat{\alpha}_s = 1$, $\alpha_d = 1/\sqrt{3}$, and the angular functions $\overline{U}_r$ and $\overline{U}_\theta$ in (13) become

$$\begin{Bmatrix} \overline{U}_r \\ \overline{U}_\theta \end{Bmatrix} = \sqrt{\frac{k_d}{2\pi}} \begin{Bmatrix} \cos\theta & \sin\theta \\ -\sin\theta & \cos\theta \end{Bmatrix} \begin{Bmatrix} \sqrt{3}\sin\frac{\theta_d}{2} \\ \cos\frac{\theta_d}{2} \end{Bmatrix}, \tag{33}$$

which do not involve any shock wave terms, where $\theta_d = \tan^{-1}\left(\frac{\tan\theta}{\sqrt{3}}\right)$, and $k_d = (1 - \frac{2}{3}\sin^2\theta)^{1/2}$. The displacements in the intermediate region in (17) become

$$\begin{Bmatrix} U_r \\ U_\theta \end{Bmatrix} = \frac{K_{\mathrm{II}}^{\mathrm{inter}}}{\mu} r^{1/2} \begin{Bmatrix} \overline{U}_r(\theta) \\ \overline{U}_\theta(\theta) \end{Bmatrix} + \begin{Bmatrix} \overline{V}_r(\theta) \\ \overline{V}_\theta(\theta) \end{Bmatrix} + \mathrm{o}(1). \tag{34}$$

The governing equations (22) for $\overline{V}_r$ and $\overline{V}_\theta$ become

$$\begin{aligned} &\frac{\mathrm{d}}{\mathrm{d}\theta}\left[\cos 2\theta\left(\overline{V}'_r - \overline{V}_\theta\right)\right] - (2+\cos 2\theta)\left(\overline{V}'_\theta + \overline{V}_r\right) = \frac{(K_{\mathrm{II}}^{\mathrm{inter}})^2}{\mu^2}\bar{f}_r(\theta), \\ &\frac{\mathrm{d}}{\mathrm{d}\theta}\left[(2+\cos 2\theta)\left(\overline{V}'_\theta + \overline{V}_r\right)\right] + \cos 2\theta\left(\overline{V}'_r - \overline{V}_\theta\right) = \frac{(K_{\mathrm{II}}^{\mathrm{inter}})^2}{\mu^2}\bar{f}_\theta(\theta), \end{aligned} \tag{35}$$

where $\bar{f}_r$ and $\bar{f}_\theta$ defined in (22) are evaluated for $v = \sqrt{2}c_{\mathrm{s}}$, and they are known in terms of the above $\overline{U}_r$ and $\overline{U}_\theta$ in (33). It is observed that (35) are linear, constant coefficient ordinary differential equations with respect to $\cos 2\theta(\overline{V}'_r - \overline{V}_\theta)$ and $(2+\cos 2\theta)(\overline{V}'_\theta + \overline{V}_r)$. Their general solutions are given by

$$\begin{aligned} (2+\cos 2\theta)\left(\overline{V}'_\theta + \overline{V}_r\right) &= C\cos\theta + D\sin\theta + \frac{(K_{\mathrm{II}}^{\mathrm{inter}})^2}{\mu^2}\int_0^\theta \left[\bar{f}'_\theta(\tau) - \bar{f}_r(\tau)\right]\sin(\theta-\tau)\,\mathrm{d}\tau, \\ \cos 2\theta\left(\overline{V}'_r - \overline{V}_\theta\right) &= C\sin\theta - D\cos\theta + \frac{(K_{\mathrm{II}}^{\mathrm{inter}})^2}{\mu^2}\bar{f}_\theta - \frac{(K_{\mathrm{II}}^{\mathrm{inter}})^2}{\pi\mu^2}\int_0^\theta \left[\bar{f}'_\theta(\tau) - \bar{f}_r(\tau)\right]\cos(\theta-\tau)\,\mathrm{d}\tau, \end{aligned} \tag{36}$$

where coefficients C and D are to be determined. For $v = \sqrt{2}c_{\mathrm{s}}$, the crack-face traction-free boundary conditions (23) become

$$\begin{aligned} &\overline{V}'_\theta + \overline{V}_r = -\frac{1}{12\pi}\frac{(K_{\mathrm{II}}^{\mathrm{inter}})^2}{\mu^2} \quad \text{at } \theta = \pm\pi, \\ &\overline{V}'_r - \overline{V}_\theta = 0 \quad \text{at } \theta = \pm\pi. \end{aligned} \tag{37}$$

The comparison of $\overline{V}'_r - \overline{V}_\theta$ in (36) and (37) yields

$$D = 0, \tag{38}$$

$$\bar{f}_\theta(\pm\pi) + \int_0^{\pm\pi}\left(\bar{f}'_\theta - \bar{f}_r\right)\cos\tau\,\mathrm{d}\tau = 0, \tag{39}$$

where we have used the fact that $\bar{f}_r$ and $\bar{f}_\theta$ are even and odd functions of θ, respectively. It can be verified that the numerical integration of $\bar{f}_r$ and $\bar{f}_\theta$ indeed satisfy (39) for $v = \sqrt{2}c_{\mathrm{s}}$. The coefficient C is determined from $\overline{V}'_\theta + \overline{V}_r$ in (36) and (37) as

$$C = \frac{(K_{\mathrm{II}}^{\mathrm{inter}})^2}{\mu^2}\left[\frac{1}{4\pi} + \int_0^\pi \left(\bar{f}'_\theta - \bar{f}_r\right)\sin\tau\,\mathrm{d}\tau\right] = 0.089\frac{(K_{\mathrm{II}}^{\mathrm{inter}})^2}{\mu^2}. \tag{40}$$

The second equation in (36) then gives

$$\overline{V}'_r - \overline{V}_\theta = \frac{(K_{\mathrm{II}}^{\mathrm{inter}})^2}{\mu^2}\frac{1}{\cos 2\theta}\left\{\bar{f}_\theta + 0.089\sin\theta - \int_0^\theta \left[\bar{f}'_\theta(\tau) - \bar{f}_r(\tau)\right]\cos(\theta-\tau)\,\mathrm{d}\tau\right\}. \tag{41}$$

Its denominator, $\cos 2\theta$, vanishes at $\theta = \pi/4$ and $3\pi/4$, while the numerator does not vanish at these two angles. Therefore, $\overline{V}'_r - \overline{V}_\theta$ are singular at $\theta = \frac{\pi}{4}$ and $\theta = \frac{3\pi}{4}$, and have $\frac{1}{\theta-\frac{\pi}{4}}$ and $\frac{1}{\theta-\frac{3\pi}{4}}$ singularities, respectively. The first equation in (36) gives $\overline{V}'_\theta + \overline{V}_r$ which is well behaved and has no singularities at $\theta = \frac{\pi}{4}$ and $\theta = \frac{3\pi}{4}$. Therefore, the integration of $\overline{V}'_r - \overline{V}_\theta$ and $\overline{V}'_\theta + \overline{V}_r$ with respect to θ gives $\overline{V}_r$ that has logarithmic singularities at $\theta = \frac{\pi}{4}$ and $\theta = \frac{3\pi}{4}$, i.e., $\ln|\theta - \frac{\pi}{4}|$ and $\ln|\theta - \frac{3\pi}{4}|$. The discontinuities in V_r both ahead of ($\theta = \frac{\pi}{4}$) and behind ($\theta = \frac{3\pi}{4}$) the crack tip are not acceptable. Therefore, $p = 2q$ and $q = \frac{1}{2}$ is not possible.

4. Discussion

The analysis in the previous section involves several assumptions and limitations. The implications of these assumptions and limitations on the conclusion of vanishing crack opening displacement for intersonic shear cracks are examined in this section. First, the stress in the outer region is on the order of r^{-q}, which neglects the higher order terms $r^{-q-1}, r^{-q-2}, r^{-q-3}, \ldots$ for an intersonic shear crack. This neglect may affect the field in the intermediate region since the field in the outer region is imposed as the remote boundary condition for the intermediate region. However, we show in the following that this neglect does not change the conclusion of vanishing crack opening displacement. It is recalled that the stress in the intermediate region is composed of three terms, (i) r^{-q}, which is the solution in the outer region; (ii) r^{-2q}, which also results from the solution in the outer region but is due to the nonlinearity in the constitutive model; and (iii) r^{-p}. Such a solution only exists for $p < 2q$ as shown in Section 3.3, and the corresponding solution for $p < 2q$ gives a vanishing crack opening displacement. Since the higher order terms $r^{-q-1}, r^{-q-2}, r^{-q-3}, \ldots$ are less dominant than r^{-2q}, the leading terms in the intermediate region remain the same as r^{-q}, r^{-2q}, r^{-p} even after the higher order terms are accounted for. Therefore, the crack opening displacement still vanishes in the intermediate region.

Secondly, the conclusion of vanishing crack opening displacement holds only in the intermediate region, not in the inner region which is in the immediate vicinity of the crack tip. In fact, we show in the following that the present constitutive model (7) based on the linear harmonic potential is not even applicable near the crack tip. This is because the well known crack tip singularity gives large shear strains near the intersonic shear crack tip, which lead to large compression in some bonds (e.g., see (5)). The linear harmonic potential (1), however, is unsuitable to large compression because it predicts a finite compressive bond force $-kl_0$ even when the bond is completely "crushed" to a vanishing bond length $l = 0$. Therefore, the constitutive model (7) based on the linear harmonic potential cannot be used to study the crack tip behavior. A nonlinear potential (e.g., the Lennard-Jones potential) which displays an infinite compressive bond force at zero bond length should be used instead.

Lastly, the present analysis neglects a finite dissipative region associated with the intersonic crack tip. Unlike a stationary or a sub-Rayleigh crack tip which has the conventional square-root singularity, an intersonic crack tip has a weaker singularity which yields a vanishing crack tip energy release rate unless there is a finite dissipative region, also known as the cohesive zone, associated with the intersonic crack tip (e.g., Kubair et al., 2002, 2003; Samudrala et al., 2002a,b). The effect of finite dissipative region is beyond the scope of the present study. Furthermore, this finite dissipative region is inconsistent with the linear harmonic potential without a cutoff distance.

5. Concluding remarks

We have extended Knowles' (1981) finite deformation analysis of static shear cracks to intersonic shear cracks in this paper. The crack tip is surrounded by an inner region, an intermediate region, and an outer region. A nonlinear and anisotropic constitutive relation is developed from a linear harmonic potential and a triangular lattice structure shown in Fig. 1. This constitutive relation is then used to study the displacement field in the intermediate region around an intersonic shear crack tip. Unlike the static shear crack (Knowles, 1981) and sub-Rayleigh dynamic shear crack (Chen et al., 2004) which have finite crack opening displacement, we have found that the intersonic shear cracks must have vanishing crack opening displacement in the intermediate region. This is consistent with Abraham and Gao's (2000) molecular dynamics simulations which showed that, under the same loading, sub-Rayleigh cracks displayed finite crack opening, while the crack opening of intersonic cracks were negligible.

Acknowledgements

Y.H. acknowledges the support from the Office of Naval Research (grant #N00014-01-1-0205, program officer Dr. Y.D.S. Rajapakse), Alexander von Humboldt Foundation, ASCI Center for Simulation of Advanced Rockets at the University of Illinois supported by US Department of Energy through the University of California under subcontract B523819, and NSFC. Y.H. and H.G. also acknowledge the support from National Science Foundation (grant #CMS0103257). W.Y. acknowledges the support from NSFC.

References

Abeyaratne, R., Knowles, J.K., 1990. On the driving traction acting on a surface of strain discontinuity in a continuum. Journal of the Mechanics and Physics of Solids 38, 345–360.

Abraham, F.F., Gao, H., 2000. How fast can cracks propagate? Physical Review Letters 84, 3113–3116.

Broberg, K.B., 1999. Cracks and Fracture. Academic Press, San Diego, California.

Chen, B., Huang, Y., Gao, H., Wu, P.D., 2004. Shear crack propagation along weak planes in solids: a finite deformation analysis incorporating the linear harmonic potential. International Journal of Solids and Structures 41, 1–14.

Freund, L.B., 1990. Dynamic Fracture Mechanics. Cambridge University Press, Cambridge, England.

Gao, H., 1996. A theory of local limiting speed in dynamic fracture. Journal of the Mechanics and Physics of Solids 44, 1453–1474.

Gao, H., Huang, Y., Abraham, F.F., 2001. Continuum and atomistic studies of intersonic crack propagation. Journal of the Mechanics and Physics of Solids 49, 2113–2132.

Gao, H., Huang, Y., Gumbsch, P., Rosakis, A.J., 1999. On radiation-free transonic motion of cracks and dislocations. Journal of the Mechanics and Physics of Solids 47, 1941–1961.

Gao, H., Klein, P., 1998. Numerical simulation of crack growth in an isotropic solid with randomized internal cohesive bonds. Journal of Mechanics and Physics of Solids 46, 187–218.

Geubelle, P.H., Knauss, W.G., 1994. Finite strains at the tip of a crack in a sheet of hyperelastic material: 1. Homogeneous case. Journal of Elasticity 35, 31–98.

Geubelle, P.H., Kubair, D., 2001. Intersonic crack propagation in homogeneous media under shear-dominated loading: numerical analysis. Journal of Mechanics and Physics of Solids 49, 571–587.

Huang, Y., Gao, H., 2001. Intersonic crack propagation—Part I: the fundamental solution. Journal of Applied Mechanics 68, 169–175.

Huang, Y., Gao, H., 2002. Intersonic crack propagation—Part II: suddenly stopping crack. Journal of Applied Mechanics 69, 76–80.

Huang, Y., Wang, Z.L., 2003. Mechanics of carbon nanotubes. In: Karihaloo, B., Ritchie, R., Milne, I. (Eds.), Comprehensive Structural Integrity Handbook. In: Gerberwich, W., Yang, W. (Eds.), Interfacial and Nanoscale Fracture, vol. 8. Elsevier Science, pp. 551–579. Chapter 8.16.

Huang, Y., Wang, W., Liu, C., Rosakis, A.J., 1999. Analysis of intersonic crack growth in unidirectional fiber-reinforced composites. Journal of Mechanics and Physics of Solids 47, 1893–1916.

Knowles, J.K., 1981. A nonlinear effect in Mode II crack problems. Engineering Fracture Mechanics 15, 469–476.

Kubair, D., Geubelle, P.H., Huang, Y., 2002. Intersonic crack propagation in homogeneous media under shear-dominated loading: theoretical analysis. Journal of Mechanics and Physics of Solids 50, 1547–1564.

Kubair, D., Geubelle, P.H., Huang, Y., 2003. Analysis of a rate-dependent cohesive model for dynamic crack propagation. Engineering Fracture Mechanics 70, 685–704.

Milstein, F., 1980. Review: theoretical elastic behavior at large strains. Journal of Material Science 15, 1071–1084.

Needleman, A., 1999. An analysis of intersonic crack growth under shear loading. Journal of Applied Mechanics 66, 847–857.

Needleman, A., Rosakis, A.J., 1999. The effect of bond strength and loading rate on the conditions governing the attainment of intersonic crack growth along interfaces. Journal of Mechanics and Physics of Solids 47, 2411–2449.

Rosakis, A.J., Huang, Y., 2003. Intersonic debonding. In: Karihaloo, B., Ritchie, R., Milne, I. (Eds.), Comprehensive Structural Integrity Handbook. In: Gerberwich, W., Yang, W. (Eds.), vol. 8. Elsevier Science.

Rosakis, A.J., Samudrala, O., Coker, D., 1999. Cracks faster than the shear wave speed. Science 284, 1337–1340.

Rosakis, A.J., Samudrala, O., Coker, D., 2000. Intersonic shear crack growth along weak planes. Materials Research Innovation 3, 236–243.

Samudrala, O., Huang, Y., Rosakis, A.J., 2002a. Subsonic and intersonic mode II crack propagation with a rate dependent cohesive zone. Journal of the Mechanics and Physics of Solids 50, 1231–1268.

Samudrala, O., Huang, Y., Rosakis, A.J., 2002b. Subsonic and intersonic shear rupture of weak planes with a velocity weakening cohesive zone. Journal of Geophysical Research—Solid Earth 107 (B8), article number 2170.

Stephenson, R.A., 1982. The equilibrium field near the tip of a crack for finite plane-strain of incompressible elastic-materials. Journal of Elasticity 12, 65–99.

Tadmor, E.B., Ortiz, M., Phillips, R., 1996. Quasicontinuum analysis of defects in solids. Philosophical Magazine A 73, 1529–1563.

Yu, H.H., Suo, Z., 2000. Intersonic crack growth on an interface. Proceedings of the Royal Society of London Series A—Mathematical. Physical and Engineering Science 456, 223–246.

Zhang, P., Huang, Y., Gao, H., Hwang, K.C., 2002a. Fracture nucleation in single-wall carbon nanotubes under tension: a continuum analysis incorporating interatomic potentials. Journal of Applied Mechanics 69, 454–458.

Zhang, P., Huang, Y., Geubelle, P.H., Hwang, K.C., 2002b. On the continuum modeling of carbon nanotubes. Acta Mechanica Sinica 18, 528–536.

Zhang, P., Huang, Y., Geubelle, P.H., Klein, P.A., Hwang, K.C., 2002c. The elastic modulus of single-wall carbon nanotubes: a continuum analysis incorporating interatomic potentials. International Journal of Solids and Structures 39, 3893–3906.